

Project No: 603502

DACCIWA

"Dynamics-aerosol-chemistry-cloud interactions in West Africa"

Deliverable

D6.3 Rainfall dataset

Due date of deliverable: 31/05/2018

Completion date of deliverable: 31/07/2018

Start date of DACCIWA project: 1st December 2013 **Project duration:** 60 months

Version: [V1.0]

File name: [D6.3_Rainfall_dataset.v1.0.pdf]

Work Package Number: 6

Task Number: 3

Responsible partner for deliverable: KIT

Contributing partners: KNUST

Project coordinator name: Prof. Dr. Peter Knippertz

Project coordinator organisation name: Karlsruher Institut für Technologie

The DACCIWA Project is funded by the European Union's Seventh Framework Programme for research, technological development and demonstration under grant agreement no 603502.

Dissemination level		
PU	Public	x
PP	Restricted to other programme participants (including the Commission Services)	
RE	Restricted to a group specified by the consortium (including the Commission Services)	
CO	Confidential, only for members of the consortium (including the Commission Services)	

Nature of Deliverable		
R	Report	
P	Prototype	
D	Demonstrator	
O	Other	x

Copyright

This Document has been created within the FP7 project DACCIWA. The utilization and release of this document is subject to the conditions of the contract within the 7th EU Framework Programme. Project reference is FP7-ENV-2013-603502.

DOCUMENT INFO

Copyright

This Document has been created within the FP7 project DACCIWA. The utilization and release of this document is subject to the conditions of the contract within the 7th EU Framework Programme. Project reference is FP7-ENV-2013-603502.

Authors

Author	Beneficiary Short Name	E-Mail
Andreas H. Fink	KIT	andreas.fink@kit.edu
Marlon Maranan	KIT	marlon.maranan@kit.edu
Joseph Njeri	KIT	joseph.njeri@kit.edu
Leonard K. Amekudzi	KNUST	leonard.amekudzi@gmail.com
Winifred A. Atiah	KNUST	winifred.a.atiah@aims-senegal.org

Changes with respect to the DoW

Issue	Comments
<p>Instead of rain gauges of tipping bucket type, rain gauges with an optical sensor have been deployed.</p> <p>The year 2015 was only partially covered by about half of the rain gauges. The network went fully operational by the end of 2015.</p> <p>Delay of the deliverable by two months due to complexity of quality control.</p>	<p>The decision to use rain gauges based on optical sensors did not significantly affect the scientific approach and output.</p> <p>In accordance to the delay of the aircraft campaign by one year to 2016, the year 2015 was not given full priority. Moreover, the focus was put on 2016 and further operation until 2018 and potentially beyond.</p> <p>Communicated to and approved by the PO with registered e-mail Ares(2018)3662098</p>

Dissemination and uptake

Target group addressed	Project internal / external
Scientific community	Internal and external

Document Control

Document version #	Date	Changes Made/Comments
0.1	04.07.2018	First draft to be commented by contributing partners
0.2	13.07.2018	Version for approval by the general assembly
1.0	31.07.2018	Final version approved by the general assembly

Table of Contents

1	Introduction	5
2	The rain gauge sites.....	6
3	Rain gauge instrumentation	7
4	Quality control and final data availability.....	8
4.1	Step 1: Removal of obvious erroneous periods.....	8
4.2	Step 2: Comparison with of individual DACCIWA RGs with GMET RGs and GPM IMERG9	
4.3	Step 3: Comparison on maps.....	11
4.4	Final data availability and rainfall patterns.....	13
5	Initial evaluation of the performance of GPM-I with daily aggregated DACCIWA RG data.....	14
6	Final remarks	17
7	References	17

1 Introduction

Sub-Saharan Africa is currently experiencing one of the strongest population, urbanisation and also economic growth on earth. According to the World Bank, the fertility rate in the region has dropped only slightly from 6.5 children in 1950-1955 to 5.4 children in 2005-2010, while child mortality and the overall life expectancy has significantly decreased and increased, respectively. Sustaining economic growth and thus the improvement of life standard and education is expected to impose a substantial demographic challenge, particularly for the already heavily urbanised region in the coastal area of West Africa. Much of the challenge is related to a sufficient drinking water, food and energy supply, which in turn is strongly dependent on rainfall. However, substantial fluctuations of rainfall on annual to decadal timescales have long been identified over West Africa, which exhibits one of the most variable climates on earth. Earlier studies on rainfall in the Savannah region of West Africa emphasise the strong contribution from so-called mesoscale convective systems (MCS), which are capable of influencing a large area over a long period of time due to their size and longevity (e.g. Fink et al., 2006). The Savannah as well as the Sahelian region have historically received a lot more attention in rainfall studies than the adjacent Guinea coast region to the south due to a massive drought and famine, which culminated in the 1980s and which was greatly covered in the media world-wide. A recent work by Maranan et al. (2018) addressed the rainfall climatology of types of rainfall in the Guinea coast region. They found that MCSs still account for the majority of rainfall in the region, but also stress the importance of less-intense convective systems due to their dominance in absolute numbers. Although this study is based on a 16-year rainfall dataset from a space-borne precipitation radar, the spatio-temporal coverage over the Guinea coast is relatively low with a maximum of six overpasses per day over the DACCIWA region. The radar also had potentially missed very small-scale but still intense rainfall systems due to limitations in spatial resolution and therefore detection. In general, deficiencies in the estimation of rainfall from space are well-known. Active measurements using the precipitation radar or microwave imagers suffer from the relatively low sample size over a specific region. The derivation of rainfall from passive infrared imagery can be quite erroneous since cold cloud-top temperatures are taken for estimation. This includes cold cloud features such as non-precipitative cirrus clouds, for instance.

To help to overcome the issue of poor ground truth data for the validation and calibration of satellite rainfall estimations, to complement existing studies and to further improve our understanding about relevant rainfall types in the Guinea coast region, a dense network of high-resolution optical rain gauges was established around the city of Kumasi in the Ashanti region of Ghana. In the following, the present report provides a detailed description of:

- the Kumasi rain gauge network,
- the instrumentation,
- the quality control and final data availability

Finally, a brief assessment of space-borne rainfall estimates with quality controlled rain gauge data is given in the last section. Note that a more thorough satellite evaluation will be described in D6.6 due on 30 November 2018.

2 The rain gauge sites

A total of 20 rain gauges (termed RGs hereafter) were manually assembled ordered in 2014 by the University of Leeds (ULEEDS), 17 of which were eventually used for operation. It was decided to keep three RGs in reserve to be able to quickly fix potential hardware malfunctions. By the time this report is compiled, components of all three spare RGs have already replaced those at several RG stations. The establishment of the RG network around Kumasi, located roughly 200 km inland of Ghana, started in June 2015 and was finished in November of that year. The spatial distribution of the RG stations as of February 2018 is illustrated in Fig. 1 (blue markers). The RGs were installed within a radius of 80 km from partner KNUST in Kumasi, who are in charge of the data collection. A substantial number of RGs were either placed in an already existing RG enclosure operated by the Ghanaian Meteorological Agency (GMET) or on a school grounds to ensure a high security standard. The locations of the RGs and collocated RGs from GMET are listed in Table 1. In essence, one fundamental aspect behind the distribution of the RGs is the capability of monitoring the movement of rainfall clouds more closely. It was ensured to provide a west-east transect to capture westward moving convective systems, particularly MCSs, which are known to be advected mostly from the east. A south-north transect was arranged to register cloud movements from the south in conjunction with the land-sea-breeze circulation. Major changes in the RG locations are confined to RG13_Airport, which was originally placed at Owabi Wildlife Sanctuary (red marker in Fig. 1). Due to the nature of this site, the RG was subject to strong environmental influences such as bigger insects and leaves, which constantly congested the funnel of the RG (see section 3) despite maintenance. In July 2017, the decision was made to relocate RG13 to the Kumasi International Airport (ICAO: DGSJ, WMO No. 65442). Here, to allow a continuation of the rainfall time series as well as the replacement of an existing recording rain gauge bucket-based RG, the latter of which went out of order and the replacement by RG13 allowed for a continuation of the high temporal resolution rainfall monitoring at Kumasi airport.

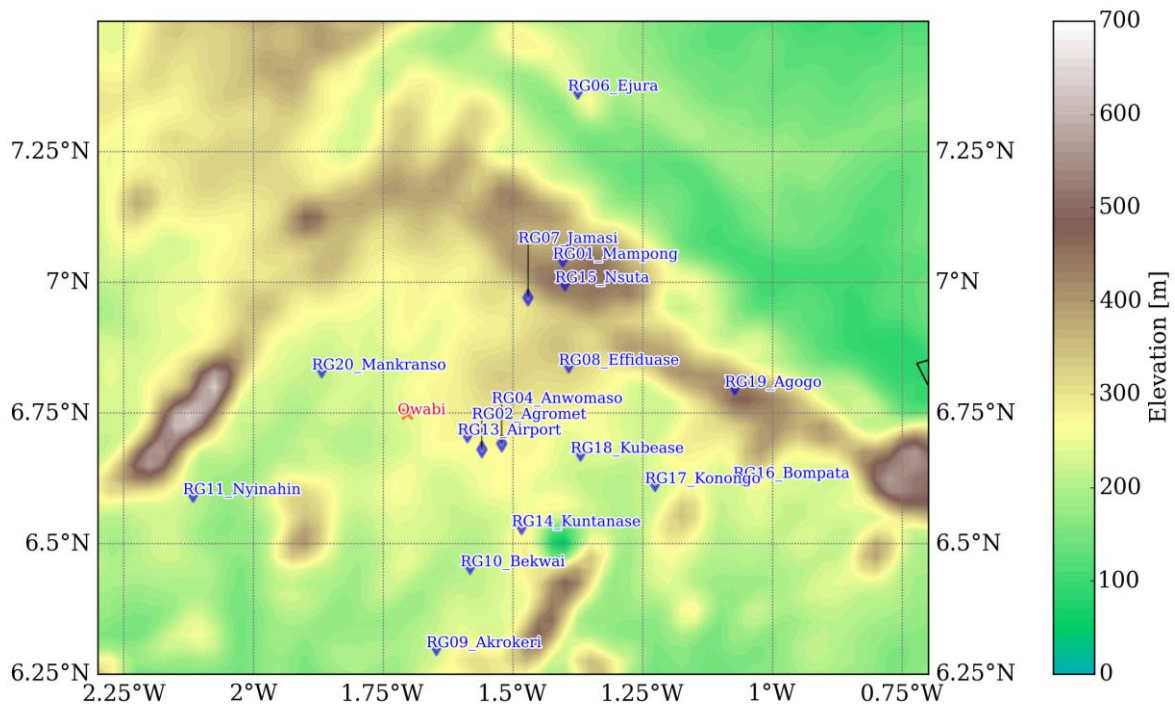


Figure 1: Station map of DACCIWA RGs (blue) in the Kumasi area as of February 2018. The location of RG02_Agromet also marks the location of the campus of KNUST. Before July 2017, RG_13 Airport was operated at the Owabi Wildlife Sanctuary (red). Colour-shaded is the terrain height.

Table 1: Meta-information about the RG stations. The numbering of the rain gauges are not continuous since three of them (RG03, RG05, RG12) are used as spare elements.

Station Name	RG Number	Longitude [E]	Latitude [N]	Elevation [m]	GMET RG available?
Mampong	RG01	-1.24	7.03	439	Yes
Agromet (KNUST)	RG02	-1.34	6.41	282	Yes
Anwomaso	RG04	-1.31	6.41	288	No
Ejura	RG06	-1.23	7.22	228	Yes
Jamasi	RG07	-1.28	6.58	316	Yes
Effiduase	RG08	-1.24	6.51	368	Yes
Akrokeri	RG09	-1.39	6.18	259	Yes
Bekwai	RG10	-1.35	6.27	241	Yes
Nyinahin	RG11	-2.07	6.35	196	No
Owabi → Airport	RG13	-1.42 → -1.59	6.45 → 6.7	237 → 287	Yes
Kuntenase	RG14	-1.29	6.32	301	No
Nsuta	RG15	-1.24	7.00	465	Yes
Bompata	RG16	-1.03	6.38	236	Yes
Konongo	RG17	-1.14	6.37	255	No
Kubease	RG18	-1.22	6.40	239	No
Agogo	RG19	-1.04	6.48	417	No
Mankranso	RG20	-1.52	6.80	243	Yes

3 Rain gauge instrumentation

The RG instrumentation consists basically of a logger box, solar panel (Fig. 2, both left) and the rainfall collector (Fig.2, right). The logger box has two main functions.

1. It controls the electricity through a solar regulator that recharges a built-in battery and switches between battery and solar panel mode, depending on which provides a higher voltage output. Either way, the rainfall collector is fed with power from both modes. Therefore, the RG forms a stand-alone system, which keeps monitoring rainfall throughout the night.
2. A microcontroller provides a Wi-Fi support, USB port and Micro SD card slot for easy data exchange. Data files are produced in the standard .csv format and are created every day at 0000 UTC. The timing is further controlled by a built-in, battery-backed and temperature compensated real-time clock, which is designed to run for approximately eight years.

The rainfall collector is mounted roughly 50 cm off the ground. It operates on the principle that rain water falling into the collector is funnelled through an orifice, which leads to the formation of drops that possess the same diameter as the orifice. For the present RGs, the diameter of the orifice as well as the cross section of the collector have been constructed such that one drop is equal to 0.01 mm. The passage of a drop is registered by an infrared sensor within the collector and causes an electric signal, which is sent back to the logger box for further data processing. The temporal resolution of data recording is one minute, which enables us to identify different rainfall types by the shape of the temporal rainfall profile. There is an upper boundary for the rainfall rate, above which the amount of collected rainfall water is too high to form single drops, but rather a stream.

This occurs approximately at 300 mm/hr. Although it is physically possible, such rainfall rates become subject to further inspection within the quality control stage (see section 4).

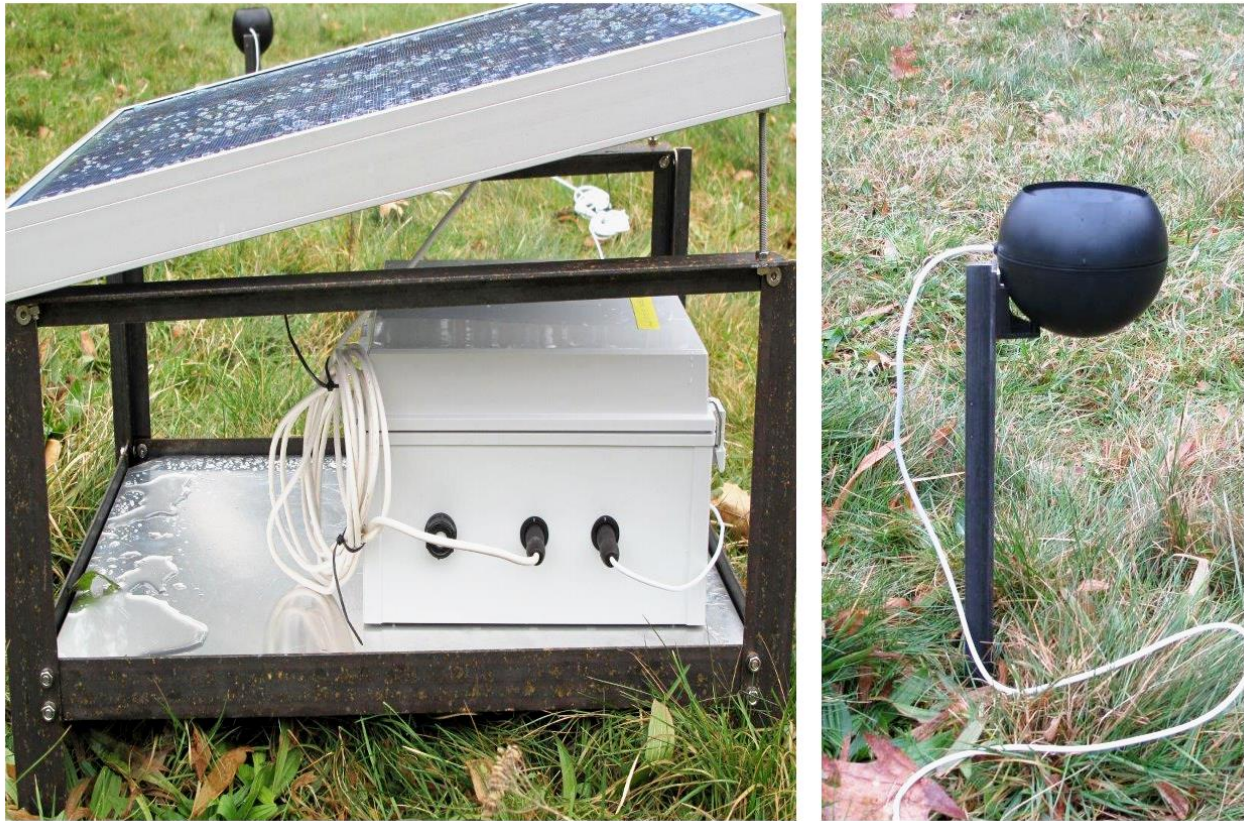


Figure 2: Rain gauge system for the DACCIWA project. (Left) Data logger box and solar panel on top. The middle socket connects the solar panel with the box, the right one the rain collector. (Right) The rain collector with the funnel on the upper side.

4 Quality control and final data availability

The quality control procedure is formed by three steps and covers the period from June 2015 to December 2017. We emphasise here that both raw and cleaned versions of the rainfall dataset will be provided to the DACCIWA community. This decision was made since particularly step 3 is predominantly based on subjective assessments, which may be judged differently by individuals.

4.1 Step 1: Removal of obvious erroneous periods

Fig. 3 shows the time series of the availability of raw data as well as the daily aggregated rainfall amount from all 17 RGs before quality control. Apparent periods without proper recordings are highlighted with red boxes, exemplarily for RG10_Bekwai and RG20_Mankranso during 2017 and 2016, respectively. The basic idea behind this very first step is the assessment of coherence among the RGs. Failed recordings over a longer period of time can be typically detected through a series of zero values. Recurrent isolated rainfall measurements within such a period were ignored and generally eliminated from the dataset. Constantly low rainfall amounts as in the case of RG20_Mankranso can be a sign of a congested rain collector that allowed only a fraction of the rain water to penetrate the system. In some cases, internal malfunctions of the rain collector (e.g. corrupted optical sensor) without visible damages also led to failed recordings (i.e. zero values). In essence, as long as the entire system is supplied with power, continuous measurements are performed. For a rain collector that is unable to send electric signals back to the logger, the rainfall amount is constantly zero. Damages on the main board inside of the logger usually lead to the same behaviour. For some periods at some stations, power outages are visible in Fig. 3 by

discontinuous bars. As mentioned, three RGs, namely RG03, RG05 and RG12, are spare elements. This simple way of detecting failed measurements is, however, only possible outside of the dry season. The rainy season over the Guinea coast region usually last from March to November. Therefore, no assessment could be made directly from December to February of a year. Finally, measurement days featuring less than 80% of daily recording are dismissed as well. However, we note that the data of these days are kept in the aforementioned raw dataset.

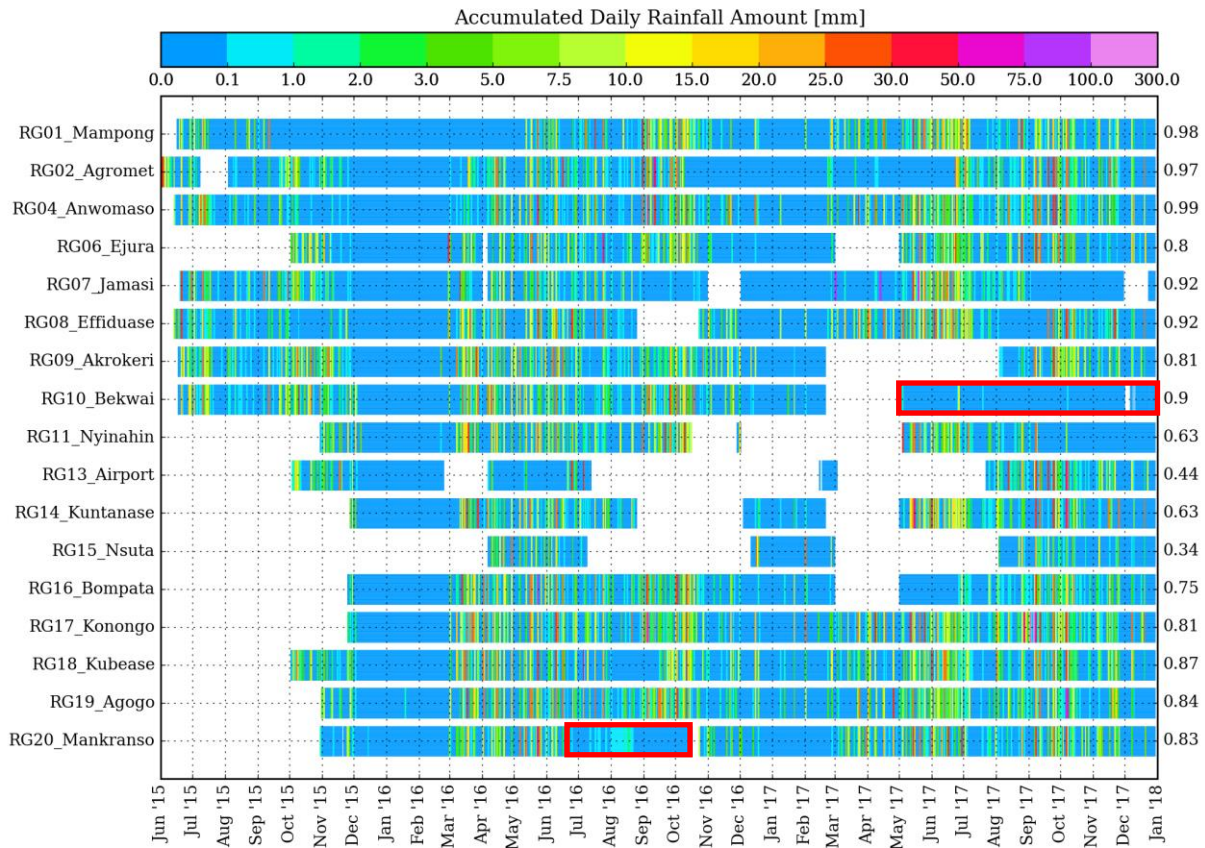


Figure 3: Data availability from June 2015 to December 2017 expressed as a horizontal bar plot. The numbers on the right axis indicate the percentage of availability in this period before quality control was performed. RG03, RG05 and RG12 are spare RGs (not listed here). Zero values are indicated in deep blue, inactive periods are blank. Color-coded is the daily accumulated rainfall. Red boxes exemplarily denote periods that were rejected during step 1.

4.2 Step 2: Comparison with of individual DACCIWA RGs with GMET RGs and GPM IMERG

The second step addresses the plausibility of the measured rainfall amounts. For this purpose, both the datasets of collocated manual GMET RGs and the space-borne rainfall estimates of the Global Precipitation Measurement (GPM) IMERG were used for the comparison with the DACCIWA RGs. To be more precise, GPM IMERG is a half-hourly, gridded ($\Delta x=0.1^\circ$) rainfall dataset, which is dedicated to the monitoring of rainfall over the tropical belt. It is termed GPM-I hereafter for the sake of simplicity. GPM-I is a blended product containing rainfall estimates from microwave and microwave-calibrated infrared retrievals. Furthermore, it is calibrated towards ground-based rain gauge data, which, as mentioned earlier, is sparse over West Africa.

The upper panels in Fig. 4 show the number distribution of binned precipitation amounts for “DACCIWA vs GMET” and “DACCIWA vs GPM-I”, respectively, exemplarily for RG06_Ejura. For GPM-I, the closest pixel to the respective RG station was taken for comparison. Ideally, the

number distribution would follow the line through origin 1:1 line (light blue dashed line), suggesting a good comparability between the datasets and high plausibility. In fact, RG06_Ejura compares well to the collocated GMET RG, as indicated by larger numbers along the 1:1 line. The cases, which strongly deviate from 1:1 line, have been subjected to further investigation described in section 4.3. For RG01_Mampong, the total hit/correct negative hit rate with GMET RG is 91.1%, i.e. both rain gauges equally detected or did not detect rainfall in 91.1% of all days. This percentage decreases for the comparison with GPM-I to 70.0%. Furthermore, the number distribution is way more scattered than with the GMET RG. However, larger differences between the DACCIWA RGs and GPM-I are not necessarily surprising on a daily basis, particularly if rainfall systems are too small-scaled to be detected by GPM-I. Generally, GMET RGs were primarily used for comparison if present, otherwise GPM-I. The bottom panels show the number distribution of the false alarm ratio (no rain detected in DACCIWA RG, but in GMET RG/GPM-I) and miss ratio (rain detected in DACCIWA RG, but none in GMET RG/GPM-I). Again, it is the larger differences that were investigated. Especially high rainfall amounts with collocated “no rain” events in the other dataset suggest inconsistencies in one the datasets. For instance, although only 1.6% are false alarms with GMET RG, the difference in the rainfall amount exceeds 30 mm on two occasions. Such cases are evaluated in section 4.3.

An extended assessment of the performance of individual DACCIWA RGs is realized by visually evaluating rainfall accumulation curves. Fig. 5 presents, amongst other, the 2016 accumulation curves of the DACCIWA RG (pink curve) and GMET RG (yellow curve), again exemplarily for RG06_Ejura. The closer the curves increase, the more consistent both datasets are among each other on a daily basis. Larger deviations between both curves were again identified. In the case of RG06_Ejura for 2016, only few periods were tested in section 4.3, for instance from day 290 onwards, where the curves start to diverge. As before, if a collocated GMET RG was not existent, GPM-I was used in the process.

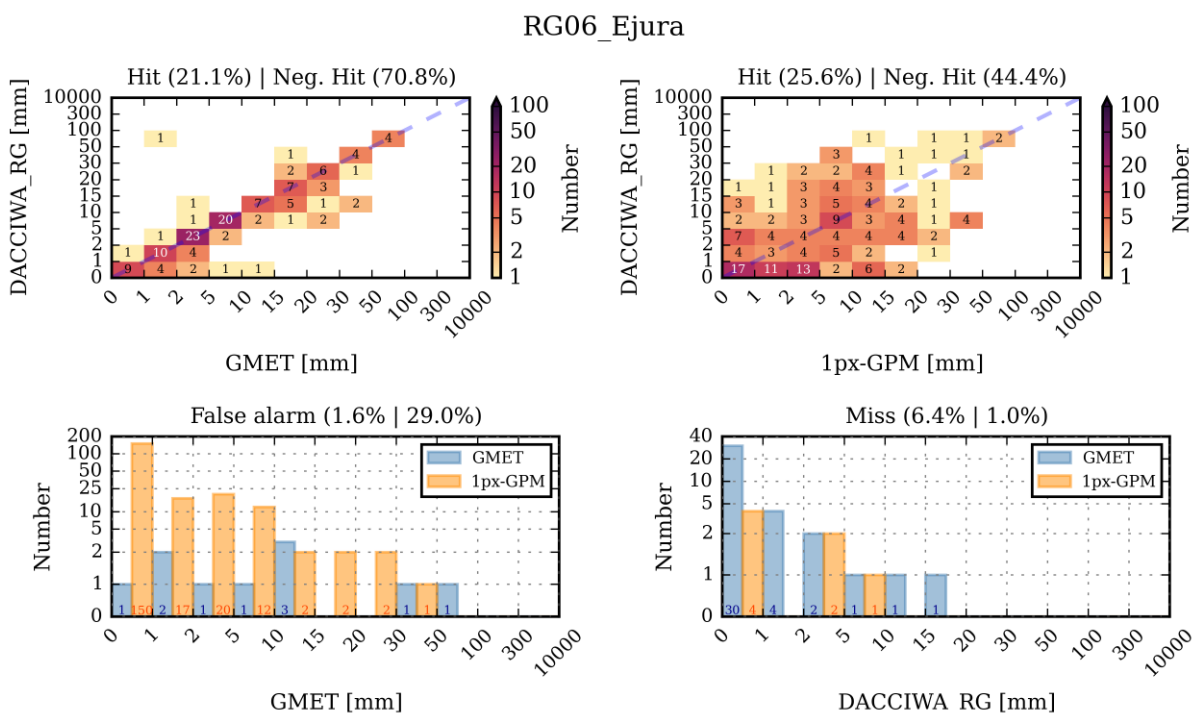


Figure 4: Comparison of daily accumulated rainfall of DACCIWA RG with GMET RG and GPM-I for RG06_Ejura for the period June 2015 to December 2017. (Upper left) Number distribution of binned daily rainfall for DACCIWA vs GMET. The 1:1 line is indicated as a light-blue dashed line. Hit (negative hit) in the title denote percentage of all days when both DACCIWA and GMET detected (did not detect) rainfall; (Upper right) DACCIWA vs GPM-I. (Bottom left) False alarm occurrences for different rainfall values, i.e. when DACCIWA registered no rain, but GMET/GPM-I did. (Bottom right) Miss rate, i.e. when DACCIWA did register rain, but GMET/GPM-I did not.

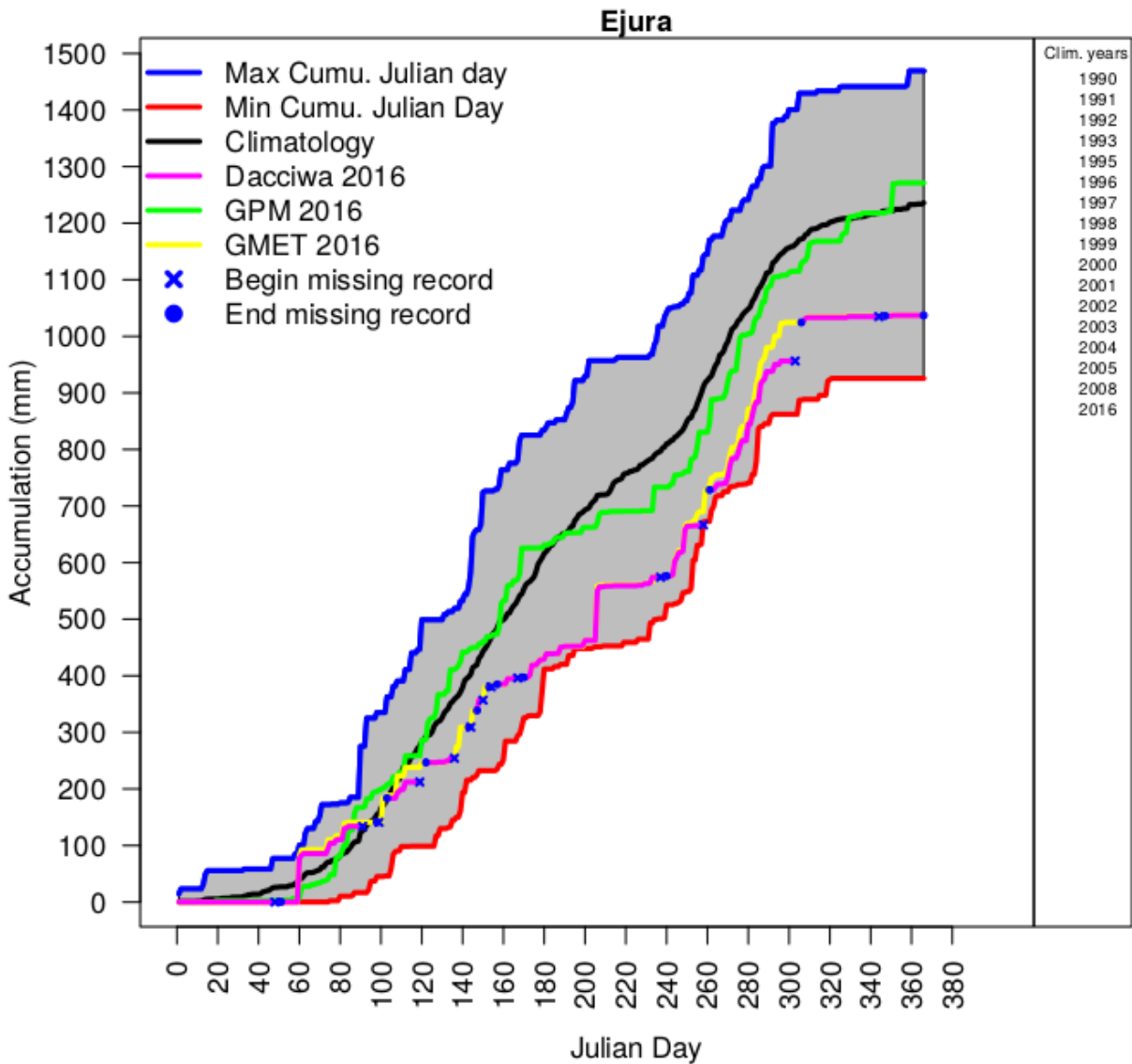


Figure 5: Rainfall accumulation curves for Ejura for 2016. The colors are assigned for the products as indicated in the legend, RG06_Ejura is pink. The years taken for calculating the climatology are indicated on the right. The envelope of the gray shaded area (blue and red line) denotes the recorded maximum and minimum accumulated rainfall at Ejura based on the KASS-D (Karlsruhe African Surface Station Database).

4.3 Step 3: Comparison on maps

In this step, the plausibility of rainfall values was subjectively assessed through spatial coherence. Fig. 6 illustrates an example for RG02_Agromet on 15 September 2016, which was dismissed. The values of available GMET RGs (scatters in left panel) and the respective DACCIWA RGs (scatters in right panel) are plotted against the GPM-I field (shaded). RG02_Agromet (dot encircled in blue) reported 32.37 mm on that day, whereas both GMET RG and GPM-I exhibit much lower values. Furthermore, there was rather little indication in surrounding DACCIWA and GMET RGs of the passage of a convective system. Although it may seem possible that a very isolated rainfall system passed RG02_Agromet, this value was rejected due to low coherence with both GMET and GPM-I. Fig. 7 shows an example for RG20_Mankranso on 24 May, 2016, where the rainfall value was kept, despite a deviation of over 30 mm to the respective GMET RG. According to GPM-I field, the

Kumasi area was passed by a convective system of larger spatial extent with both stations exceeding 100 mm on that day. This is a case where no binary conclusion could be made about the validity of both rainfall values. Again, the decision-making was highly subjective and non-trivial in many cases. The quality controlled dataset serves as a recommendation, but can still be overthrown by using the original dataset.

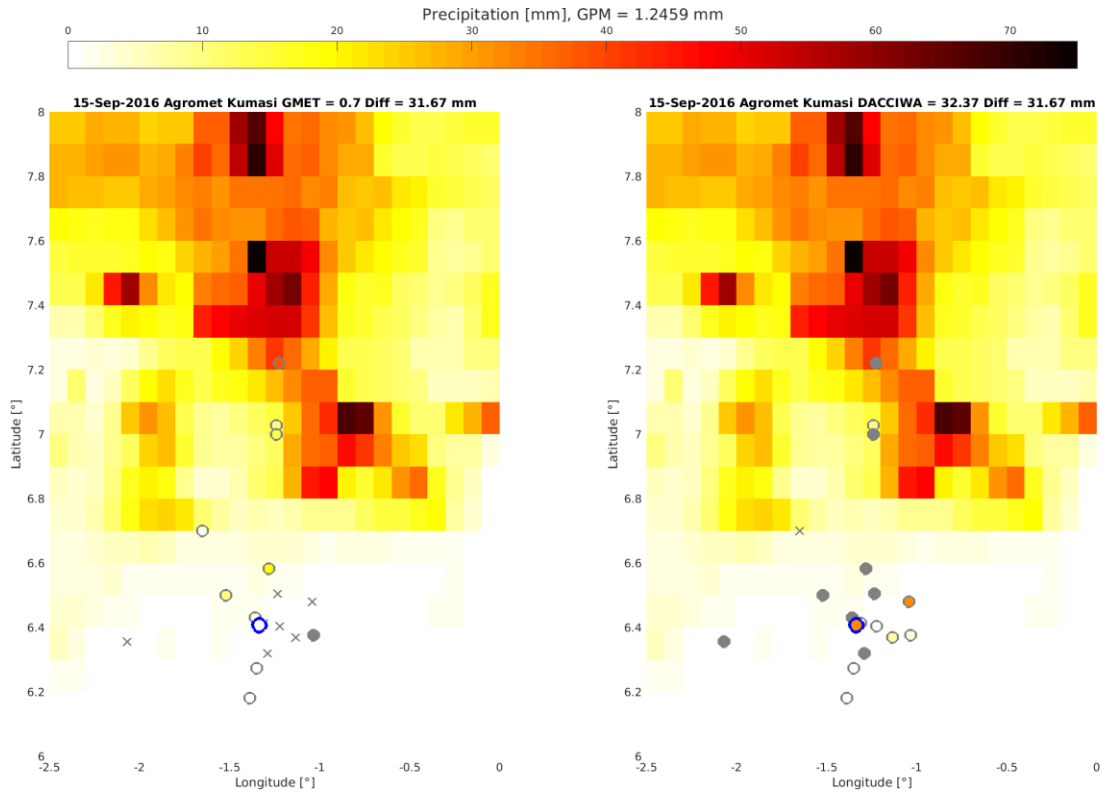


Figure 6: Accumulated rainfall on 15 September 2016 for the GMET RGs (scatters in the left panel) and DACCIWA RGs (scatters in the right panel), each against GPM-I (color shaded). The RGs at Agromet are encircled blue. The absolute rainfall values for GMET and DACCIWA at Agromet are indicated in the respective titles, together with the difference DACCIWA-GMET. The absolute value at the respective GPM-I pixel is indicated at the colorbar.

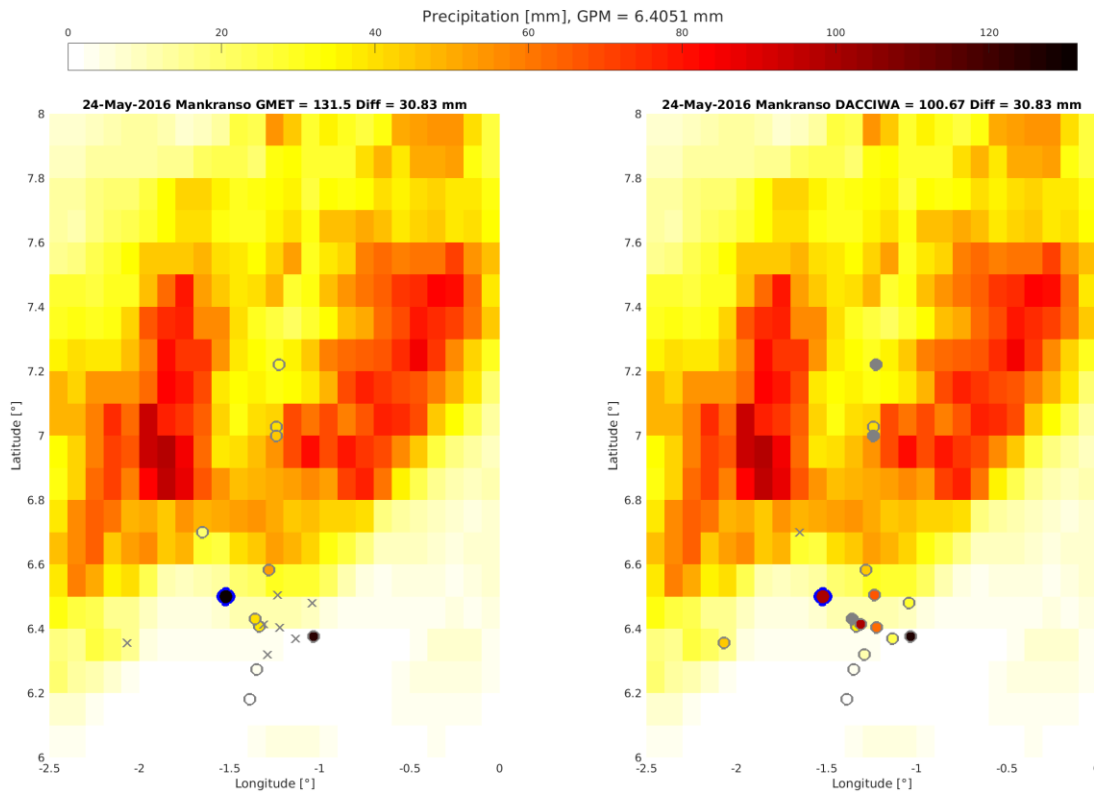


Figure 7: Same as Figure 6, but for RG20_Mankranso on 24 May 2016

4.4 Final data availability and rainfall patterns

Having performed step 1-3 of the quality control, the final time series of data availability is presented in Fig. 8. Compared to Fig. 3, step 1 had the largest impact since entire periods were dismissed. Step 2 and 3 addressed mostly individual days and are hardly visible in Fig. 8. Overall, between June 2015 and December 2017, the availability of non-relocated stations ranges from 45% at RG11_Nyinahin to 99% at RG04_Anwomaso. We note that some stations were established in November 2015. For these stations, the maximum percentage of availability in the aforementioned period is naturally lower at around 80% (e.g. RG19_Agogo). Care must be taken with RG13_Airport. As stated in section 2, the RG was relocated from Owabi to the Kumasi Airport. Therefore, the data in 2015/2016 for RG13_Airport is assigned to the Owabi site. Several features of the West African Monsoon (WAM) are clearly evident from the dataset. The dry season over the Kumasi area sets in in December and lasts to March. It is particularly pronounced in 2015/2016 where very few weak rainfall days were registered. Accordingly, the rainy season starts around March and lasts to October/November. It is interrupted by the little dry season during July and August, where days with zero rainfall increase.

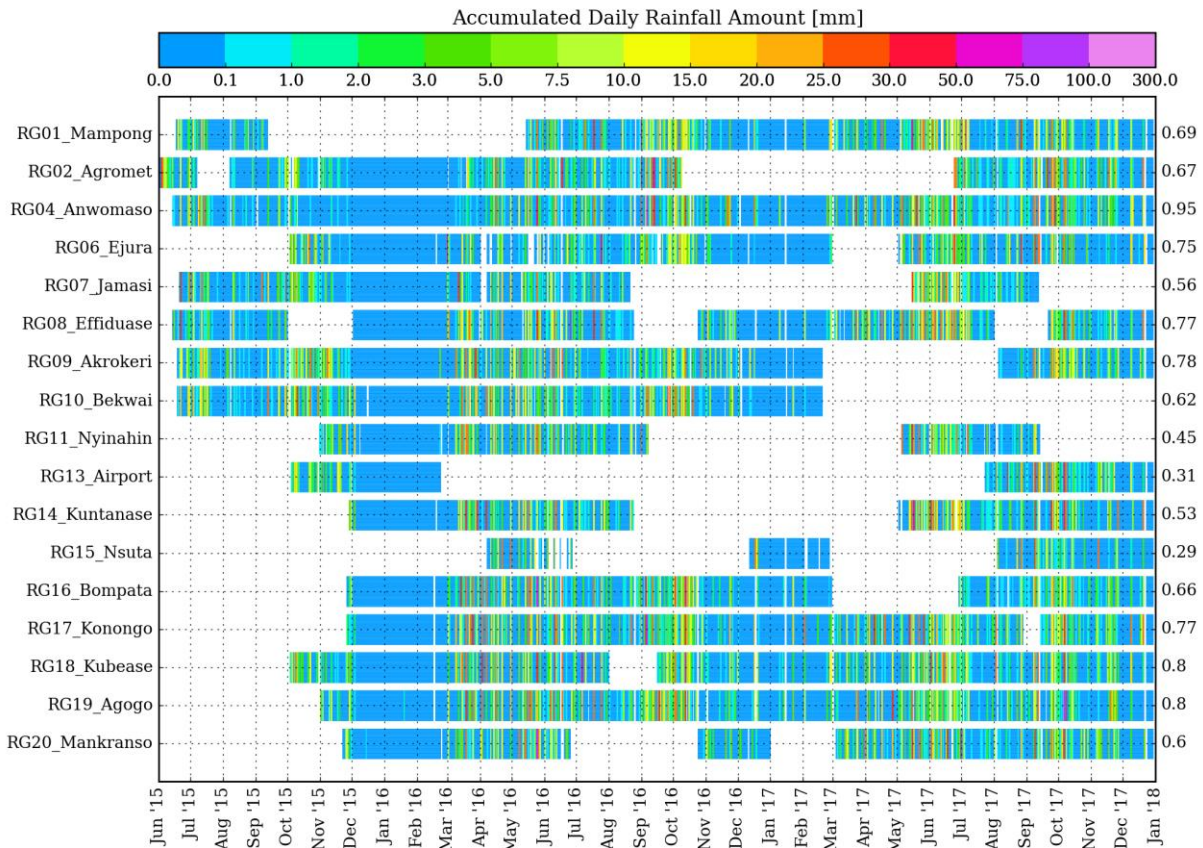


Figure 8: Same as Figure 3, but after the quality control.

5 Initial evaluation of the performance of GPM-I with daily aggregated DACCIWA RG data

In the following, we briefly present an initial performance test of the GPM-I using the daily aggregated data of the DACCIWA RGs. We refer to section 4.2 for some more details about GPM-I. A more detailed assessment of the quality of satellite retrievals will be given in the upcoming deliverable D6.6. Both the DACCIWA RG and GPM-I datasets were aggregated from 0900 UTC to 0900 UTC the next day and follows the philosophy of GMET. The Taylor diagram in Fig. 9 provides a summary of the relative skill of GPM-I to “reproduce” the rainfall at the pixel of the respective DACCIWA RG, exemplarily for RG19_Agogo. We refer to the entire dataset available between June 2015 and December 2017. Three statistics are plotted:

1. Pearson correlation: The Pearson correlation is indicated as the “zenith angle” and is a measure of pattern similarity between GPM-I pixel and the RG on a daily basis. For RG19_Agogo, we obtain a value of 0.55. In fact, a correlation coefficient of 0.5 ± 0.1 for daily rainfall is a typical value across all stations (see Table 2). This is not too surprising given the relative vicinity of DACCIWA RG stations to each other within the network and thus sharing a similar climatological rainfall zone. It remains to investigate to what extent the correlation coefficient is controlled by different types of rainfall systems in the Guinea coast region. For instance, we expect convective systems of large extent to be captured by GPM-I, whereas it is generally known that satellites experience difficulties to detect small-scale rainfall systems, which could lower the correlation coefficient.
2. Standard deviation: For GPM-I, this metric is related to the radial distance from the origin point. For the GPM-I pixel over RG19_Agogo, the standard deviation is 6.8 mm during the

entire measurement period. Compared to the standard deviation of the station (9.8 mm), which is indicated by the thick yellow line and/or the squared marker, the standard deviation of GPM-I is smaller by 3 mm. This means that GPM-I underestimates the variation in daily rainfall values of the station measurement. This is true for the majority of the stations (Table 2). Again, possible reasons for this will be evaluated in one of the upcoming deliveries.

3. Centred root mean square error (CRMSE): The CRMSE relative to the station observation is given by the radial distance from the yellow squared marker and indicates the RMSE from the station observation after the bias has been removed (also called unsystematic error). For the GPM-I pixel over RG19_Agogo, the CRMSE is 7.9 mm and is again a typical value over the ensemble of DACCIWA RGs. Overall, GPM-I appears to perform homogeneously across the entire network as indicated by the relatively low variation in CRMSE among the DACCIWA RG stations ($8.1 \text{ mm} \pm 1.4 \text{ mm}$).

Larger deviations from the general pattern are visible for RG15_Nsuta (Fig. 10). GPM-I shows the lowest correlation coefficient with 0.33 and overestimates the variation in daily rainfall by 1.8 mm (see also Table 2). However, as seen in Fig. 8, RG15_Nsuta has one of the shortest data records and hardly covered the rainy season in the measurement period. Therefore, the assessment of GPM-I based on RG15_Nsuta is less robust.

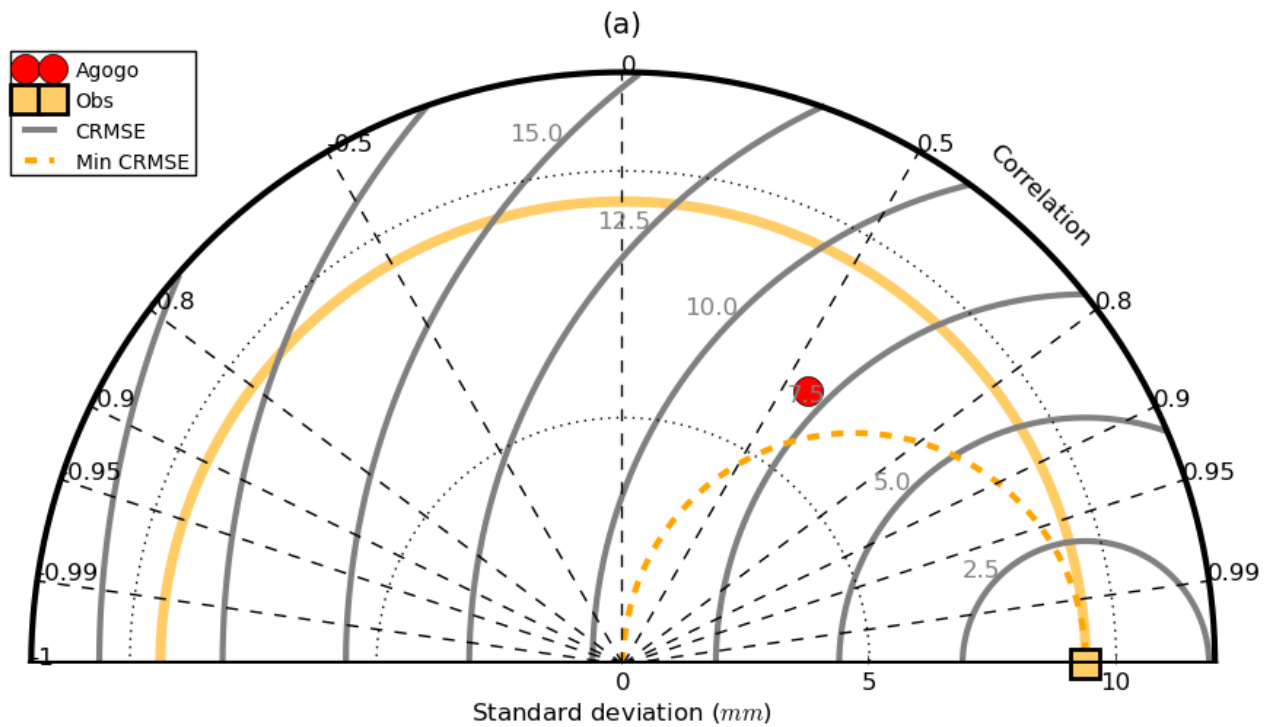


Figure 9: Taylor diagram summarising the performance of GPM-I relative to RG19_Agogo. The three metrics displayed are: correlation coefficient (dashed lines), standard deviation (dotted lines) and centred root mean square error (thick gray lines). The position of the red dot (i.e. GPM-I) indicates the value for the three metrics. The yellow line denotes the standard deviation within RG19_Agogo.

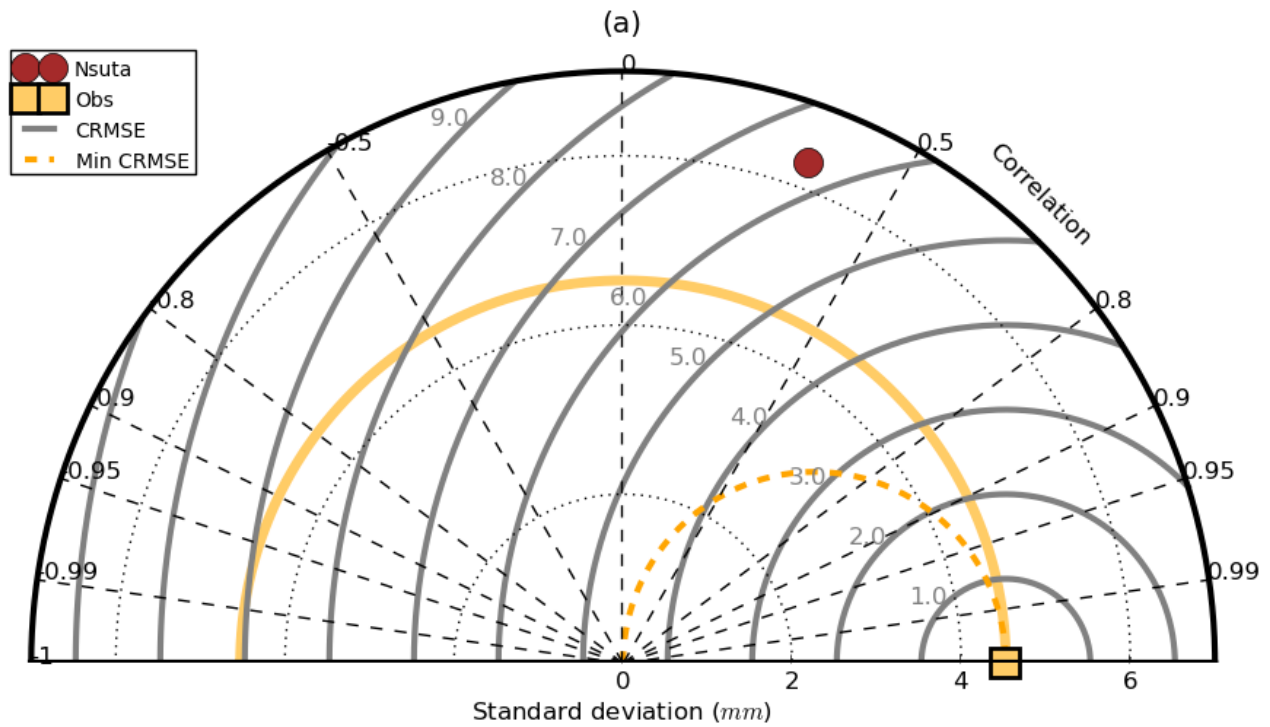


Figure 10: Same as Fig. 9, but for RG15_Nsuta.

Table 2: Results of the metrics from the Taylor diagram (see Figure 9, 10) for all stations. RG13_Airport was omitted due to relocation and consequently a too short measuring period.

Station Name	RG Number	r	σ (GPM-I) [mm]	σ (RG) [mm]	CRMSE [mm]
Mampong	RG01	0.66	7.03	439	9.5
Agromet (KNUST)	RG02	0.48	7.5	9.4	8.8
Anwomaso	RG04	0.40	7.5	9.4	9.3
Ejura	RG06	0.60	6.4	7.7	6.6
Jamasi	RG07	0.53	7.6	7.7	7.5
Effiduase	RG08	0.52	7.5	8.8	8.0
Akrokeri	RG09	0.55	7.2	7.2	6.8
Bekwai	RG10	0.47	7.8	8.4	8.5
Nyinahin	RG11	0.66	8.1	8.3	6.8
Owabi → Airport	RG13	---	---	---	---
Kuntense	RG14	0.53	7.2	10.3	8.8
Nsuta	RG15	0.33	6.2	4.4	6.3
Bompata	RG16	0.41	6.4	10.0	9.5
Konongo	RG17	0.51	6.9	10.2	9.2
Kubease	RG18	0.52	7.5	9.2	8.3
Agogo	RG19	0.55	6.8	9.8	7.9
Mankranso	RG20	0.48	7.3	9.2	8.6

6 Final remarks

With the quality-checked data of 17 stations and the high temporal resolution of one minute, a unique dataset has been provided to the DACCIWA and general research community that will allow ground-breaking analysis of rainfall systems and evaluation of satellite rainfall estimates in the hitherto under-gauged Guinea coastal regions with its rainfall climate different to the regions farther north. As mentioned, some further exploration of the performance of GPM-I and other satellite rainfall estimations in comparison to the DACCIWA RG network will be executed. This will also comprise the analysis of sub-daily rainfall data to exploit the high temporal resolution of both the DACCIWA RG (one minute) and GPM-I (30 minutes).

For the DACCIWA community, two types of rainfall datasets will be made available on the Baobab server:

- The cleaned, quality-controlled dataset in .txt format, which is recommended for usage. Data will be provided on a daily and minutely basis. For the latter, the consequences of the above-described quality controls have yet to be applied to the raw data. According to national Ghanaian standards, the daily rainfall is measured in the period 0900 – 0900 UTC, thus all rainfall intensities in mm/minute on days flagged as erroneous have to be removed from the data set. These data set will be uploaded shortly.
- The raw rainfall datasets on a minutely basis in the csv format in the way they are produced by the data logger. They are not quality-controlled. However, measuring days that were dismissed during the quality control process are retained.

7 References

Fink, AH., Vincent, D., & Ermert, V. (2006). Rainfall types in the West African Sudanian zone during the summer monsoon 2002. *Monthly Weather Review*, pp. 2143-2164.

Maranan, M., Fink, AH., & Knippertz, P. (2018). Rainfall types over southern West Africa: Objective identification, climatology and synoptic environment. *Q. J. Royal Meteorol. Soc.*, doi:10.1002/qj.3345.